

Two-Dimensional (2D) Pulsed Electron Paramagnetic Resonance Study of VO²⁺–Triphosphate Interactions: Evidence for Tridentate Triphosphate Coordination, and Relevance To Bone Uptake and Insulin Enhancement by Vanadium Pharmaceuticals

Sergei A. Dikanov,^{*,†,‡} Barry D. Liboiron,[§] and Chris Orvig^{*,§}

Contribution from the Illinois EPR Research Center and Department of Veterinary Clinical Medicine, 190 MSB, 506 South Mathews Avenue, University of Illinois at Urbana-Champaign, Urbana, Illinois 61801, Institute of Chemical Kinetics and Combustion, Russian Academy of Sciences, Novosibirsk 6300090, Russia, and Medicinal Inorganic Chemistry Group, Department of Chemistry, University of British Columbia, 2036 Main Mall, Vancouver, BC, Canada, V6T 1Z1

Received May 1, 2001. Revised Manuscript Received January 14, 2002

Abstract: Two- and four-pulse electron spin echo envelope modulation (ESEEM) and four-pulse two-dimensional hyperfine sublevel correlation (HYSCORE) spectroscopies have been used to determine the solution structure of a 3:1 triphosphate:vanadyl solution at pH 5.0. Limited quantitative data were extracted from the two pulse spectra; however, HYSCORE proved to be more useful in the detection and interpretation of the ³¹P and ¹H couplings. Three sets of cross-peaks were observed for each nucleus. For the ³¹P couplings, three sets of cross-peaks were observed in the HYSCORE spectrum, and contour line shape analysis yielded coupling constants of approximately 15, 9, and 1 MHz. HYSCORE cross-peaks in the proton region were partially overlapping; however, interpretation of the proton coupling was simplified through the use of one-dimensional four-pulse ESEEM and subsequent analysis of the sum combination peaks. Comparison of the derived isotropic and anisotropic coupling constants with results from earlier ESEEM and electron nuclear double resonance (ENDOR) studies was consistent with the presence of at least one, and most likely two, water molecules coordinated in the equatorial plane of the vanadyl cation. The vanadyl–triphosphate system was shown to be an accurate model of the in vivo vanadyl-phosphate coupling constants determined in an earlier study (Dikanov, S. A.; Liboiron, B. D.; Thompson, K. H.; Vera, E.; Yuen, V. G.; McNeill, J. H.; Orvig, C. *J. Am. Chem. Soc.* **1999**, *121*, 11004.) Comparison of these values to those found in previous spectroscopic studies of vanadyl–triphosphate interactions, along with a detailed structural interpretation, are presented. This work represents the first detection of tridentate polyphosphate coordination to the vanadyl ion, and the first observation of an axial phosphate interaction not previously reported in earlier ENDOR and pulsed electron paramagnetic resonance studies.

Introduction

Vanadium is a ubiquitous ultra-trace element which has many effects within biological systems. In recent years, much work has focused on the accurate delineation of its effects in vivo, with the goals of describing the mechanisms of action that lead to the observed antimitotic¹ or antidiabetic² effects of various vanadium species. Toward this end, the development of a metabolic model for administered vanadium is an important goal

in our laboratories. While there have been several pertinent studies,^{3–6} the description of the absorption, transport, accumulation, and elimination of the two main biologically relevant vanadium oxidation states (IV and V) is not yet complete. Such studies would be particularly relevant because vanadyl,^{7,8} vanadate,⁹ and bis(ethylmaltolato)oxovanadium(IV) (BEOV) have all proceeded to Phase I clinical trials in recent

* To whom correspondence should be addressed in the Illinois EPR Research Center (S.A.D.): Tel, (217)-333-3776; Fax, (217)-333-8868; E-mail, dikanov@uiuc.edu. In the Department of Chemistry, UBC (C.O.): Tel, (604)-822-4449; Fax, (604)-822-2847; E-mail, orvig@chem.ubc.ca.

[†] University of Illinois at Urbana-Champaign.

[‡] Russian Academy of Sciences.

[§] University of British Columbia.

(1) Djordjevic, C. *Met. Ions Biol. Syst.* **1995**, *31*, 595.

(2) Thompson, K. H.; McNeill, J. H.; Orvig, C. *Chem. Rev.* **1999**, *99*, 2561.

(3) Harris, W. R.; Friedman, S. B.; Silberman, D. *J. Inorg. Biochem.* **1984**, *20*, 157.

(4) Kustin, K.; Robinson, W. E. *Met. Ions Biol. Syst.* **1995**, *31*, 511.

(5) Fantus, I. G.; Tsiani, E. *Mol. Cell. Biochem.* **1998**, *182*, 109.

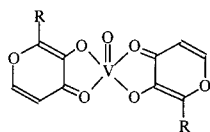
(6) Cam, M. C.; Brownsey, R. W.; McNeill, J. H. *Can. J. Physiol. Pharmacol.* **2000**, *78*, 829.

(7) Cohen, N.; Halberstam, M.; Shlimovich, P.; Chang, C. J.; Shamooh, H.; Rossetti, L. *J. Clin. Invest.* **1995**, *95*, 2501.

(8) Halberstam, M.; Cohen, N.; Shlimovich, P.; Rossetti, L.; Shamooh, H. *Diabetes* **1996**, 659.

(9) Goldfine, A. B.; Simonson, D. C.; Folli, F.; Patti, M.-E.; Kahn, C. R. *J. Clin. Endocrinol. Metab.* **1995**, *80*, 3311.

years. Vanadium-containing insulin-mimetic agents represent a potentially significant advance over currently available diabetes therapies.²



R = CH₃: Bis(maltolato)oxovanadium(IV), BMOV
R = CH₂CH₃: Bis(ethylmaltolato)oxovanadium(IV), BEOV

Previously, the ⁴⁸V-labeled insulin-enhancing complex bis(maltolato)oxovanadium(IV) (BMOV) was used in comparison with ⁴⁸VOSO₄ to elucidate the pharmacokinetics of an orally administered vanadium drug.¹⁰ This study showed that, for either V compound, accumulation took place preferentially in bone, liver, and kidneys, concomitant with rapid clearance from the bloodstream. These results led us to attempt to describe the in vivo coordination structure of the paramagnetic vanadium(IV) in these tissues¹¹ using one- and two-dimensional electron spin-echo envelope modulation (ESEEM), following an earlier reported work by Fukui et al.¹² In each of these studies, tissue samples were taken from rats which had been treated chronically with oral doses of BEOV¹¹ or VOSO₄.¹² Of particular interest in our study was the detection of three distinct ³¹P hyperfine coupling constants (15, 9, 3 MHz) from phosphates in bone. It was clear that the vanadyl ions had adopted a new coordination environment, having lost the original ethylmaltolato ligands at some point post-administration. These experiments were unable to determine, however, whether the signals arose from a single distinct vanadyl complex, ligated by three distinct phosphate groups, or from a superposition of signals from multiple vanadyl complexes present in the bone mineral. We have therefore endeavored to describe the in vivo coordination through the use of model complexes.

In this paper, we present a complete ESEEM and hyperfine sublevel correlation (HYSCORE) characterization of the 3:1 L:M solution of triphosphate and vanadyl ion as a probe into the in vivo coordination structure of vanadyl ions in bone and of divalent metal ion interactions with polyphosphate chains. Detailed analysis of the ¹H and ³¹P cross-peaks of the HYSCORE spectra indicates tridentate coordination of the triphosphate ligand and equatorial solvent coordination. A weak axial phosphate P—O coordination precludes water coordination to the sixth position trans to the V=O bond, a feature not previously detected in other studies of vanadyl-triphosphate and vanadyl-nucleotide interactions. Our study indicates that the current understanding of the coordination of divalent metal ions to triphosphate chains may require revision to account for this facial polyphosphate coordination.

Vanadyl ions have seen extensive use as spin probes in biological systems. The VO²⁺ cation, with a d¹ electron configuration, typically possesses axial hyperfine and *g* tensors, useful in the structural characterization of the paramagnetic

species. Electron paramagnetic resonance (EPR) methods, such as ESEEM, HYSCORE, and electron nuclear double resonance (ENDOR) spectroscopies, have been very useful in elucidating the structures of metal binding sites of numerous metalloenzymes and macromolecules.^{13–16} Considerable interest has focused on the interaction of VO²⁺ with polyphosphate chains as models for the interactions of Mg²⁺ with important biomolecules, such as nucleotides. In delineating the solution structure of VO-ATP complexes, the coordination site of any solvent (water) molecules relative to the V=O bond is of considerable importance. Previous work using ¹H ENDOR strongly suggested only axial solvent coordination, and the formation of a bis(ATP) complex, with no coordination to the adjacent ribose or adenine base moieties.¹⁷ Many studies have focused on the 2:1 complex due to its dominance (according to potentiometric results) at physiological pH, but the interaction of single triphosphate chains with metal ions has greater relevance to the in vivo situation. Intracellular polyphosphate binding of vanadyl ions may also protect the VO²⁺ from hydrolysis and further redox activity,¹⁸ and these ligands are important potential binding sites for intracellular vanadium in their own right.¹⁹

Experimental Section

Pentasodium triphosphate was obtained from Sigma and used without modification. Vanadium atomic absorption standard solution (in 5% HCl) was obtained from Aldrich and carefully neutralized to pH 1.0 with 10% NaOH solution. Vanadyl concentrations were confirmed by titration against potassium permanganate.

VO²⁺-Triphosphate Sample (VO-TPH). Pentasodium tripolyphosphate (0.0606 g, 0.127 mmol) and vanadyl stock solution (2.0 mL of 1.808 × 10⁻² M, 0.036 mmol) were combined and diluted to 50.0 mL with degassed, distilled, deionized water. The solution was kept under Ar and stirred for 20 min; the pH was adjusted to 5.0 by slow, dropwise addition of 0.1 M NaOH. Glycerol (21 mL, 30 vol %) was added, and the solution was stirred for a further 30 min. An aliquot of this solution was then loaded into a 4 mm i.d. quartz cryotube for spectroscopic study. The triphosphate to VO²⁺ ratio was 3.1:1.

EPR Measurements. The continuous wave (CW) EPR and ESEEM experiments were carried out using X-band Bruker ESP-380E and Bruker EleXsys E580 spectrometers equipped with Oxford CF 935 cryostats, at 25 K. Several types of ESEEM experiments with different pulse sequences were employed; among those used were the two-pulse and both 1D and 2D four-pulse sequences. The intensity of the echo signal in the two-pulse experiment ($\pi/2$ - τ - π - τ -echo) is measured as a function of the time interval τ between two microwave pulses with turning angles $\pi/2$ and π . In the 2D four-pulse experiment ($\pi/2$ - τ - $\pi/2$ - t_1 - π - t_2 - $\pi/2$ - τ -echo),²⁰ also called HYSCORE, the intensity of the stimulated echo after the fourth pulse is measured with t_2 and t_1 varied, and τ constant. Such a 2D set of echo envelopes gives, after complex Fourier transformation, a 2D spectrum with equal resolution in each direction. This procedure differs from the 1D version of the four-pulse

- (10) Setyawati, I. A.; Thompson, K. H.; Yuen, V. G.; Sun, Y.; Battell, M.; Lyster, D. M.; Vo, C.; Ruth, T. J.; Zeisler, S.; McNeill, J. H.; Orvig, C. *J. Appl. Physiol.* **1998**, *84*, 569.
(11) Dikanov, S. A.; Liboiron, B. D.; Thompson, K. H.; Vera, E.; Yuen, V. G.; McNeill, J. H.; Orvig, C. *J. Am. Chem. Soc.* **1999**, *121*, 11004.
(12) Fukui, K.; Ohya-Nishiguchi, H.; Nakai, M.; Sakurai, H.; Kamada, H. *FEBS Lett.* **1995**, *368*, 31.

- (13) Hamstra, B. J.; Houseman, A. L. P.; Colpas, G. J.; Kampf, J. W.; LoBrutto, R.; Frasch, W. D.; Pecoraro, V. L. *Inorg. Chem.* **1997**, *36*, 4866.
(14) Houseman, A. L. P.; Morgan, L.; LoBrutto, R.; Frasch, W. D. *Biochemistry* **1994**, *33*, 4910.
(15) Dikanov, S. A.; Tyryshkin, A. M.; Hüttermann, J.; Bogumil, R.; Witzel, H. *J. Am. Chem. Soc.* **1995**, *117*, 4976.
(16) Goldfarb, D.; Bernardo, M.; Thomann, H.; Kroneck, P. M. H.; Ullrich, V. *J. Am. Chem. Soc.* **1996**, *118*, 2686.
(17) Mustafa, D.; Telsler, J.; Makinen, M. W. *J. Am. Chem. Soc.* **1992**, *114*, 6219.
(18) Woltermann, G. M.; Scott, R. A.; Haight, G. P. *J. Am. Chem. Soc.* **1974**, *96*, 7569.
(19) Buglyó, P.; Kiss, T.; Alberico, E.; Micera, G.; Dewaele, D. *J. Coord. Chem.* **1995**, *36*, 105.
(20) Höfer, P.; Grupp, A.; Nebenführ, H.; Mehring, M. M. *Chem. Phys. Lett.* **1986**, *132*, 279.

experiment where the time τ between first and second pulses is kept constant and the times $t_1 = t_2 = T/2$ are increased stepwise.²¹

The length of the $\pi/2$ pulse was 16 ns. A four step phase cycle, $+(0,0,0,0)$, $-(0,0,0,\pi)$, $+(0,0,\pi,0)$, $-(0,0,\pi,\pi)$, was used to eliminate unwanted features from experimental echo envelopes.²¹ HYSORE data were collected as 2D time-domain patterns containing 256×256 points with a step of 16 ns. Spectral processing of ESEEM patterns was performed using Bruker WIN-EPR software.

Characteristics of HYSORE Spectra from $I = 1/2$ Nuclei. The most informative experimental data regarding the ligand environment of VO-TPH were obtained from the 2D ESEEM (HYSORE) experiment.²⁰ The basic advantage of the HYSORE technique is the creation in 2D spectra of off-diagonal cross-peaks whose coordinates are nuclear frequencies from opposite electron spin manifolds. The cross-peaks simplify significantly the analysis of congested spectra by correlating and spreading out the nuclear frequencies.²² In addition, the HYSORE experiment separates overlapping peaks along a second dimension and enhances the signal-to-noise ratio through the application of a second Fourier transform.^{20,22}

HYSORE spectra are sensitive to the relative signs of the correlated frequencies and are usually presented as two quadrants (+,+) and (+,-). A nucleus with $I = 1/2$, such as ¹H and ³¹P, has two hyperfine frequencies, ν_α and ν_β , which may produce one pair of cross-features, (ν_α, ν_β) and (ν_β, ν_α) , in the (+,+) quadrant as well as another pair, $(\nu_\alpha, -\nu_\beta)$ and $(\nu_\beta, -\nu_\alpha)$, in the (+,-) quadrant. Peaks in the (+,-) quadrant appear primarily for strong hyperfine interactions, that is, $|T + 2a| \gg 4\nu_1$, while the peaks in the (+,+) quadrant appear predominantly for $|T + 2a| \ll 4\nu_1$ (where a is the isotropic hyperfine coupling, T is the perpendicular component of the axial anisotropic hyperfine tensor, and ν_1 is the nuclear Zeeman frequency). Peaks may appear in both quadrants simultaneously if the hyperfine and Zeeman couplings are comparable.²³ Orientationally disordered (i.e., powder) spectra of $I = 1/2$ nuclei also provide the visualization of interdependence between ν_α and ν_β belonging to the same orientations in the form of cross-peak contour projection. The analysis of the contour allows for the direct, simultaneous determination of the nuclear isotropic and anisotropic hyperfine coupling constants.²⁴

Results

EPR/ESEEM. CW EPR and field-sweep ESE spectra of the frozen VO-TPH solution showed a spectrum with axially symmetric g -tensor anisotropy $g_\perp = 1.983 \pm 0.005$, $g_\parallel = 1.92 \pm 0.01$ and ⁵¹V hyperfine structure A_\parallel (⁵¹V) = 20.2 mT, A_\perp (⁵¹V) = 8.3 mT, typical for square pyramidal oxovanadium(IV) complexes.^{25,26} The spectral line shape was characteristic of isolated VO²⁺ species; no polynuclear phosphate species were detected.

Figure 1 shows the modulus FT two-pulse ESEEM spectrum of VO-TPH measured at the $m_1^V = -1/2$ component of the hyperfine structure from ⁵¹V. The distinctive feature of this component in X-band EPR is the close proximity of singularities corresponding to the perpendicular and parallel orientations of the external magnetic field to the unique axis of the ⁵¹V hyperfine tensor. This leads to the line shape of this component resembling more a single peak in contrast to other components

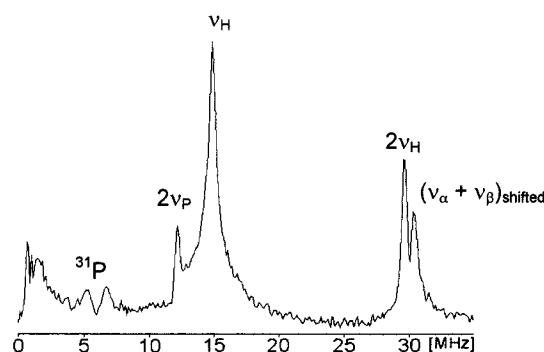


Figure 1. Modulus two-pulse ESEEM spectrum measured at the maximum intensity of the $m_1^V = -1/2$ peak of the EPR spectrum of VO-TPH (magnetic field 347.9 mT, microwave frequency 9.713 GHz).

which possess extended line shapes typical for an axially symmetric hyperfine tensor with well-separated parallel and perpendicular singularities.²⁷ Therefore, one can consider the excitation of the $m_1^V = -1/2$ component as essentially nonselective and exploit ESEEM spectral analysis approaches normally used for orientationally disordered (i.e., powder) systems.

The spectrum depicted in Figure 1 exhibits discernible features which allow some preliminary quantitative conclusions to be made about the vanadyl coordination. These features include the doublet of lines at 6.7 and 5.3 MHz centered relative to the Zeeman frequency of ³¹P, $\nu_P = 6.00$ MHz, and the peak of a sum combination harmonic at 30.35 MHz shifted to the higher frequencies relative to the proton double Zeeman frequency $2\nu_H = 29.62$ MHz.

The doublet of lines indicates ³¹P nucleus(i) with hyperfine coupling of $\sim 1-1.5$ MHz within the VO²⁺ surroundings. Such splitting cannot result from interactions with randomly distributed, remote ³¹P nuclei, which produce a single line at the Zeeman frequency of phosphorus, and, therefore, the direct coordination of at least one phosphate to the metal ion can be inferred. There is also a peak in the low-frequency region of the spectra with a maximum at ~ 1.5 MHz. This peak may be a result of other ³¹P nuclei, strongly coupled with the VO²⁺ unpaired electron, although its exact source is not obvious from the one-dimensional spectrum. The presence of sum combinations with a shift of ~ 0.7 MHz at a field strength of ~ 330 mT is typical of equatorial water coordination to vanadyl.^{28,29} Thus, analysis of the two-pulse spectrum provides the first indications of mixed coordination of VO²⁺ by phosphate and water molecules. More complete information about the phosphorus and proton environments of the vanadyl ions was obtained from the application of more sophisticated 1D and 2D ESEEM approaches.

HYSORE. Contour HYSORE spectra of VO-TPH are shown in Figures 2 and 3. The spectrum in Figure 2a, defined between -18 and $+12$ MHz in one dimension and 0 and 15 MHz in the second, contains three different pairs of cross-peaks, designated P₁, P₂, and P₃. The low intensity cross-peaks P₁ appear in the (+,-) quadrant with a maximum at frequencies $\sim [\pm 1.8; \mp 13.5]$ MHz, oriented approximately parallel to the diagonal and centered at 8 MHz. The difference between the

(21) Gemperle, C.; Aebli, G.; Schweiger, A.; Ernst, R. R. *J. Magn. Reson.* **1990**, *88*, 241.
 (22) Dikanov, S. A. In *New Advances in Analytical Chemistry*; Atta-ur-Rahman, Ed.; Gordon and Breach: Amsterdam, 2000; p 523.
 (23) Dikanov, S. A.; Tyryshkin, A. M.; Bowman, M. K. *J. Magn. Reson.* **2000**, *144*, 228.
 (24) Dikanov, S. A.; Bowman, M. K. *J. Magn. Reson., Ser. A* **1995**, *116*, 125.
 (25) Chasteen, N. D. In *Biological Magnetic Resonance*; Berliner, L. J., Reuben, J., Eds.; Plenum Press: New York, 1981; Vol. 3, pp 53-119.
 (26) Cornman, C. R.; Geiser-Bush, K. M.; Rowley, S. P.; Boyle, P. D. *Inorg. Chem.* **1997**, *36*, 6401.

(27) Grant, C. V.; Cope, W.; Ball, J. A.; Maresch, G.; Gaffney, B. J.; Fink, W.; Britt, R. D. *J. Phys. Chem. B* **1999**, *103*, 10627.
 (28) Tyryshkin, A. M.; Dikanov, S. A.; Evelo, R. G.; Hoff, A. J. *J. Chem. Phys.* **1992**, *97*, 42.
 (29) Tyryshkin, A. M.; Dikanov, S. A.; Goldfarb, D. *J. Magn. Reson., Ser. A* **1993**, *105*, 271.

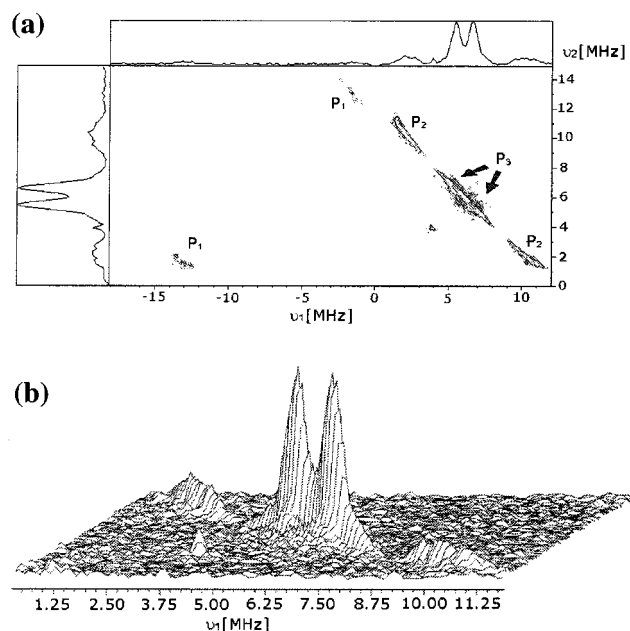


Figure 2. (a) The fragment of the contour 2D ESEEM spectrum showing the phosphorus cross-peaks P_1 – P_3 . The spectrum was measured at the maximum intensity of the $m_I^V = -1/2$ peak of the EPR spectrum of VO–TPH (magnetic field 347.9 mT, $\tau = 120$ ns, microwave frequency 9.713 GHz). (b) Stacked plot presentation of the (+,+) quadrant of spectrum a.

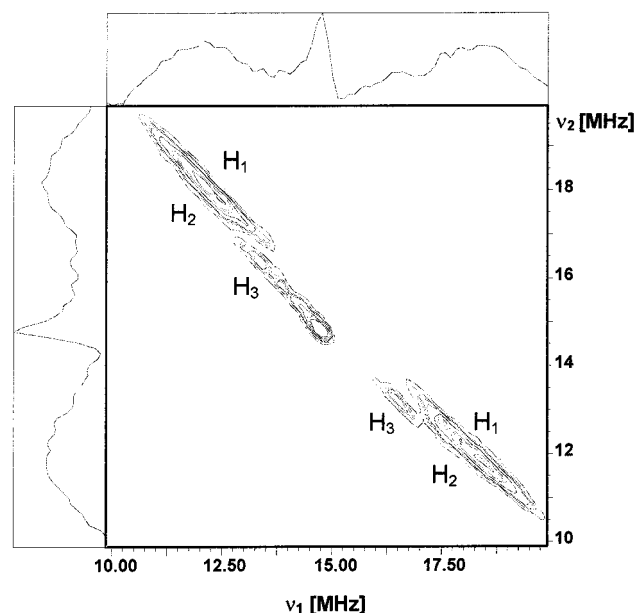


Figure 3. The fragment of the contour 2D ESEEM spectrum showing the proton cross-peaks H_1 – H_3 . The spectrum was measured at the maximum intensity of the $m_I^V = -1/2$ peak of the EPR spectrum of VO–TPH.

two coordinates of each peak is close to double the Zeeman frequency of ^{31}P ($2\nu_P$). The two other cross-features P_2 and P_3 are located in the (+,+) quadrant. They appear as extended narrow ridges between [10.1; 2.2] MHz and [7.0; 5.0] MHz, plus a pair of peaks at [6.5; 5.5] MHz with a small coupling of ~ 1 MHz centered symmetrically around the diagonal point of $\nu_P = 6.00$ MHz. The latter peaks are also shown more clearly in the stacked plot presentation in Figure 2b. The location and properties of the observed cross-peaks lead to their assignment as three different vanadyl-phosphorus couplings of ~ 15 , 9, and 1 MHz, respectively. The clear observation of lines possessing

the small coupling of 1 MHz was facilitated by the absence of a diagonal peak from weakly coupled matrix nuclei at the phosphorus Zeeman frequency in this sample.

In addition to the phosphorus lines, the spectra possess a group of strong lines grouped around the intense diagonal peak corresponding to the proton Zeeman frequency $\nu_H = 14.8$ MHz (Figure 3). There is a pair of clearly resolved cross-peaks labeled H_1 which extend between [18.8; 11.5] and [16.5; 13.9] MHz, with a maximum at [17.8; 12.3] MHz in this particular spectrum. The extended features of cross-peak H_1 are distorted asymmetrically along the bottom ridge, possibly a result of the close proximity of the intense peaks of H_1 with lower intensity H_2 lines. This interpretation is supported by an observation of proton sum combination lines in 1D four-pulse ESEEM spectra (vide infra). The final pair of cross-peaks (H_3) is located close to the diagonal. One of the cross-features of H_3 is found to be partially overlapped by the proton matrix peak centered at the diagonal, despite careful selection of τ to suppress strongly the matrix signal.

Analysis of HYSORE Spectra. The contour line shape in the powder 2D spectrum from the ^1H and ^{31}P nuclei (both with nuclear spin $I = 1/2$) for axial hyperfine interactions is described by eq 1.²⁴

$$\nu_\alpha = \{Q_\alpha \nu_\beta^2 + G_\alpha\}^{1/2} \quad (1)$$

where

$$Q_\alpha = \frac{T + 2a - 4\nu_I}{T + 2a + 4\nu_I}$$

and

$$G_\alpha = 2\nu_I \left(\frac{4\nu_I^2 - a^2 + 2T^2 - aT}{T + 2a + 4\nu_I} \right)$$

The square of each pair of cross-peak frequencies can be plotted as ν_α^2 versus ν_β^2 , transforming the contour line shape into a straight line segment whose slope and intercept are proportional to Q_α and G_α , respectively. These values can then be used to obtain simultaneously two possible sets of isotropic (a) and anisotropic (T) couplings.

The coordinates (ν_α , ν_β) of arbitrary points along the top ridge forming each cross-peak (either ^1H or ^{31}P) were measured from HYSORE spectra recorded with different τ values at a constant magnetic field value (corresponding to the maximum of the $m_I^V = -1/2$ peak) and plotted in the coordinates ν_α^2 versus ν_β^2 as shown in Figures 4 and 5. The obtained points have been fitted using a linear regression with slopes and intercepts given in Table 1.

Included with the experimental points, the curve $|\nu_\alpha + \nu_\beta| = 2\nu_I$ (for ν_I corresponding to ν_P or ν_H) is plotted in Figures 4 and 5 for ^{31}P and ^1H , respectively. The points at which the curve crosses each extrapolated straight line correspond to the nuclear frequencies at canonical orientations. They define the range of possible frequencies in powder spectra for each nucleus at this particular value of ν_I . These canonical frequencies can also be used to determine the hyperfine parameters. For an axial hyperfine tensor, there are two possible assignments of the parallel or perpendicular orientations and consequently two sets of hyperfine tensors, one for each assignment. This approach

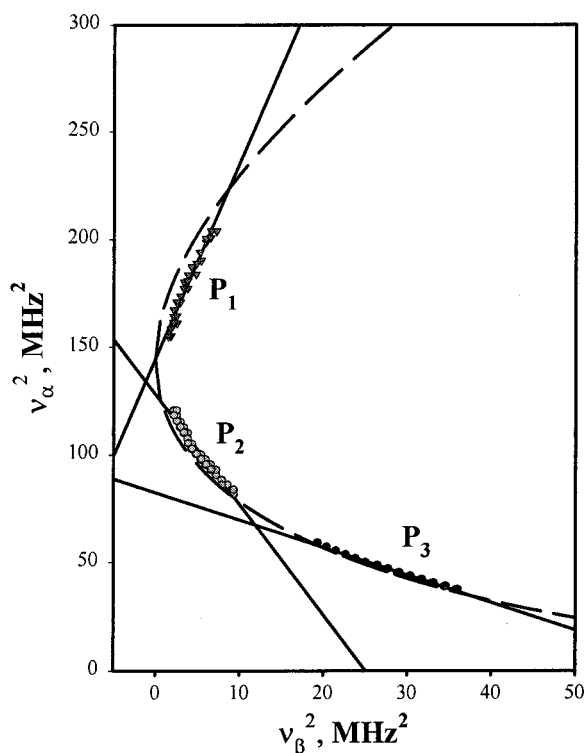


Figure 4. Points of cross-peaks P₁–P₃ from HYSORE spectra measured at different τ in the ν_α^2 vs ν_β^2 coordinate system. The larger coordinate of each point is arbitrarily chosen as ν_α , and the smaller coordinate is chosen as ν_β . The straight lines show the linear fit of plotted data points. The dashed line is defined by $|\nu_\alpha + \nu_\beta| = 2\nu_p$ with $\nu_p = 6.00$ MHz.

gives hyperfine couplings identical to those determined from the slope and intercept. The placement of this curve on each figure (Figures 4 and 5) provides additional evidence for the correct assignment of these peaks to protons and phosphorus. The measured points fit to the linear regression with a high degree of accuracy and are found in the proper region relative to this curve, as the extrapolated regression line crosses the curve at two points. These intercepts would not be observed if the signals originated with other elements.

Additionally, the crossing of the regression lines with the curve $|\nu_\alpha + \nu_\beta| = 2\nu_l$ provides evidence that peaks P₁–P₃ and H₁–H₃ belong to different nuclei. It has been shown that for strongly nonaxial hyperfine tensors, up to three separate ridges (even observed in both quadrants) may appear in the HYSORE spectrum.²³ The regression lines of such ridges must form a triangle with the apexes on the $|\nu_\alpha + \nu_\beta| = 2\nu_l$ curve; however, the regression lines in Figures 4 and 5 do not form such a shape, indicating three different types of nuclei with hyperfine tensors well described by the axial approximation.

One can point out, however, an increasing deviation from linearity of the points forming the ridges of the H₁ cross-peaks, which might indicate contributions from protons with different coupling constants. Our estimates, based on the presentation of these peaks as a superposition of two lines, lead to an assignment of the couplings with a spread of $a = \pm 2$ MHz and the same T value of about 4.3 MHz. It may be suggested that other additional factors may disturb the line shape of cross-peaks and contribute to the observed deviations of the experimental points from the straight contour described by eq 1. Such factors might be g -tensor anisotropy, anisotropy of hyperfine tensor, accuracy of determination of the (ν_α, ν_β) coordinates from the discrete

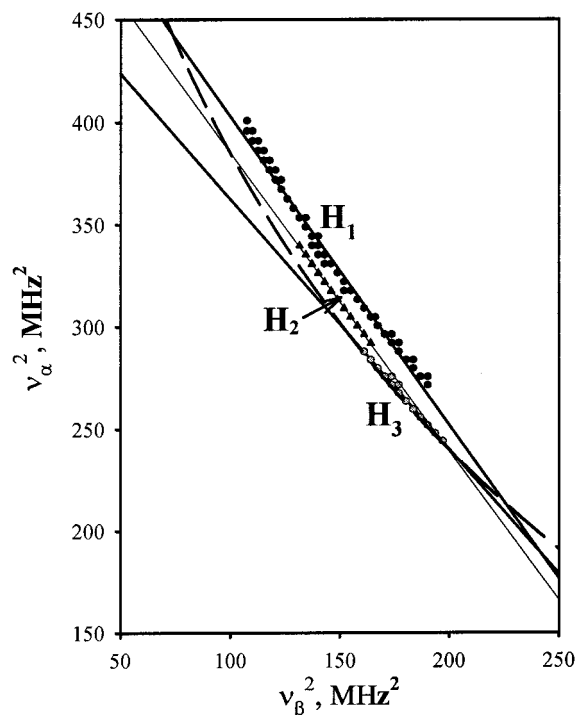


Figure 5. Points of cross-peaks H₁–H₃ from HYSORE spectra measured at different τ in the ν_α^2 vs ν_β^2 coordinate system. The larger coordinate of each point is arbitrarily chosen as ν_α , and the smaller coordinate is chosen as ν_β . The straight lines show the linear fit of plotted data points. The dashed line is defined by $|\nu_\alpha + \nu_\beta| = 2\nu_H$ with $\nu_H = 14.81$ MHz.

character of the 2D data acquisition, and spectral distortions associated with the data collection over the limited time interval.

Sum Combination Lines in ESEEM Spectra. Additional information about the proton environment of vanadyl in the VO–TPH complex, and support for our line assignment in the HYSORE spectra, were obtained from the observation of proton sum combination lines in two- and four-pulse experiments. Two- and four-pulse ESEEM spectra of VO–TPH contain lines in the region of single and double Zeeman proton frequencies from protons located in the surroundings of the VO²⁺ ion. Previous ESEEM studies of [VO(H₂O)₅]²⁺ in powder and glassy solution have shown that sum combination peaks, shifted relative to the matrix line at $2\nu_H$, appear from protons of ligand molecules.^{28,29}

The two-pulse ESEEM spectrum of VO–TPH (Figure 1) clearly showed the existence of at least one line shifted to higher frequencies relative to the proton $2\nu_H$ line (at 29.62 MHz), but resolution in this region was incomplete because of a relatively fast decay limited by the electronic relaxation time T_2 . The use of a one-dimensional four-pulse sequence, with the echo decay time limited by the much longer relaxation time T_1 , allowed improved resolution. The four-pulse ESEEM spectrum of VO–TPH contains three well-resolved lines in the region of the proton $2\nu_H$, shown in Figure 6. One of the lines appears exactly at the $2\nu_H$ frequency and therefore represents the matrix protons. The second line is shifted to higher frequencies similar to the signal observed in the two-pulse spectrum. The four-pulse spectrum, however, revealed a new weak peak with a smaller shift relative to $2\nu_H$ that was not observed in the two-pulse spectrum.

In powder ESEEM spectra the frequency of the sum combination harmonic maximum (ν_+) from an $I = 1/2$ nucleus

Table 1. Parameters Derived from Contour Lineshape Analysis of HYSCORE Spectra^a

cross-peak	Q_{α}	G_{α} , MHz ²	a , MHz	$ T $, MHz
P ₁	9.09 (0.38)	144.74 (1.50)	-15.90 (0.2)/14.0 (0.05)	1.94 (0.18)
P ₂	-5.11 (0.15)	128.07 (0.85)	-8.82 (0.03)/7.33 (0.18)	1.48 (0.16)
P ₃	-1.27 (0.02)	82.39 (0.54)	-2.01 (0.1)/0.88 (0.25)	1.14 (0.3)
H ₁	-1.51 (0.02)	554.04 (2.36)	-8.17 (0.16)/3.87 (0.2)	4.29 (0.05)
H ₂	-1.46 (0.01)	531.66 (1.8)	-6.9 (0.3)/4.15 (0.08)	2.79 (0.03)
H ₃	-1.2256 (0.03)	485.21 (4.6)	-3.66 (0.3)/2.39 (0.32)	1.22 (0.03)

^a Values in parentheses represent standard errors.

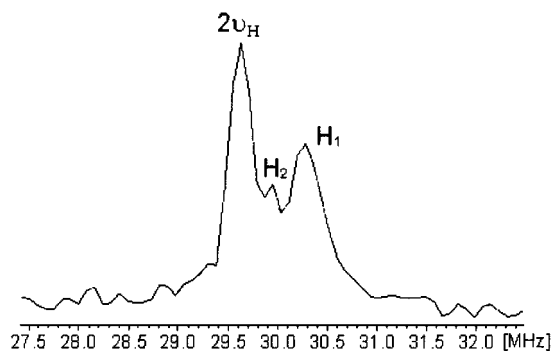


Figure 6. Proton sum combination peaks in the 1D four-pulse ESEEM spectrum (magnetic field 347.9 mT, $\tau = 120$ ns, microwave frequency 9.713 GHz).

(proton in this case) with hyperfine couplings a and T is described by eq 2.³⁰

$$\nu_{+} = 2\nu_{\text{H}} \left[1 + \frac{9T^2}{16\nu_{\text{H}}^2 - (T + 2a)^2} \right]^{1/2} \quad (2)$$

The shifts $\Delta = \nu_{+} - 2\nu_{\text{H}}$ calculated for the parameters a and T obtained from the analysis of the contour line shapes of the cross-peaks H₁–H₃ (Table 1) are equal to 0.73, 0.32, and 0.06 MHz, respectively. The two largest calculated shifts agree with the shifts of the two lines resolved in the four-pulse spectrum shown in Figure 6. The third shift is too small to be resolved, even in a four-pulse spectrum. Thus, the observation and analysis of proton sum combination peaks confirm the assignment made in the HYSCORE spectra for the proton(s) H₂ which produce peaks that are strongly overlapped by the intense peaks of the H₁ protons.

Discussion

Previous investigations into the coordination of triphosphate chains to the vanadyl cation have provided only incomplete descriptions of the metal ion coordination. Two previous characterizations using potentiometry and electron paramagnetic resonance in aqueous solution drew different conclusions regarding the formation of mono- and bis(triphosphate) species.^{19,31} Triphosphate forms relatively strong complexes with vanadyl, protecting the cation from hydrolysis above pH 7.5. Cini et al.³¹ found only monoligand complexes at $2.5 \leq \text{pH} \leq 6.5$. They quote a [(VO)L] species with $\log \beta = 9.87$ and [(VO)HL] (where L = P₃O₁₀⁵⁻) with $\log \beta = 14.06$. At pH 5.0, over 90% of the VO²⁺ would be present as the former species. The pK_a of the ligand proton would therefore be 4.29, which suggests coordination of the third phosphate moiety. Kiss, Micera, and

co-workers¹⁹ described formation of two bisligand species ([(VO)L₂H] and [(VO)L₂]) at pH > 4, in addition to the two previously proposed mono complexes, by utilizing EPR techniques in conjunction with potentiometric analysis. Using this method, they were able to detect bis(ligand) species not previously reported by Cini et al. At pH 5.0, however, over 80% of the vanadyl ion would still be present as a monoligand species. It should be noted that they invoke a tridentate triphosphate ligand bound to the vanadyl ion, due to a ligand deprotonation with a pK_a = 3.87, in reasonable agreement to the deprotonation step discussed in the earlier work.³¹ The pK_a's of TP_H³⁻ and TP_H⁴⁻ (i.e., the last two ionizable protons of the free ligand) were determined to be 5.36 and 7.78, respectively, clearly indicating the effect of the coordinated metal ion on the acidity of these protons. Analysis of EPR spectra also agreed with tridentate chelation by the fully deprotonated triphosphate, based on small differences in g and A tensors. On the basis of these earlier studies, the pH of the VO–TPH solution was set at 5.0 where the concentration of 1:1 vanadyl:triphosphate species was maximized. Additionally, at that particular pH, both previous studies indicated that the largest concentration component was a fully deprotonated vanadyl–triphosphate species, which would allow for the possible detection of a tricoordinate triphosphate ligand.

Much work has also been conducted on the related VO–ATP system.^{32–35} ATP possesses three potential metal binding sites, the triphosphate chain, the C-3 and C-4 hydroxyls of the ribose moiety, and the nitrogens of the adenine base. Potentiometric results, in combination with EPR spectra, indicate that vanadyl is bound by the phosphate chain in acidic to neutral media, but coordinated to the ribose in alkaline solution.³⁶ The 1:1 complex below pH 6 is thought to involve bidentate coordination by the γ - and β -phosphates of the triphosphate chain.

Phosphorus Couplings. Two-dimensional ESEEM spectra of VO–TPH show the presence of three ³¹P couplings with significantly distinct isotropic hyperfine constants. The derived hyperfine couplings of VO–TPH can be compared with the phosphorus couplings observed in vanadyl–adenosine complexes.^{17,37} EPR titration, based on the measurement of the peak-to-peak intensity of one component of the spectrum, indicated a 1:2 metal:ligand stoichiometry for ADP and ATP, with vanadyl chelation occurring via the phosphate groups.¹⁷ EPR spectra of [VO(ADP)₂]⁻ in frozen solution exhibit additional

(30) Reijerse, E. J.; Dikanov, S. A. *J. Chem. Phys.* **1991**, *95*, 836.

(31) Cini, R.; Giorgi, G.; Laschi, F.; Sabat, M.; Sabatini, A.; Alberto, V. J. *Chem. Soc., Dalton Trans.* **1989**, 575.

(32) Etcheverry, S. B.; Ferrer, E. G.; Baran, E. J. *Z. Naturforsch.* **1989**, *44b*, 1355.

(33) Sakurai, H.; Goda, T.; Shimomura, S. *Biochem. Biophys. Res. Commun.* **1982**, *108*, 474.

(34) Urretavizcaya, G.; Baran, E. J. *Z. Naturforsch.* **1987**, *42b*, 1537.

(35) Williams, P. A. M.; Baran, E. J. *Inorg. Biochem.* **1992**, *48*, 15.

(36) Alberico, E.; Dewaele, D.; Kiss, T.; Micera, G. *J. Chem. Soc., Dalton Trans.* **1995**, 425.

(37) Buy, C.; Matsui, T.; Andrianambininstoa, S.; Sigalat, C.; Girault, G.; Zimmerman, J.-L. *Biochemistry* **1996**, *35*, 14281.

hyperfine structure assigned to four equivalent phosphorus nuclei with a hyperfine coupling constant of 18.54 MHz.¹⁷ This result suggests that the equatorial coordination of the phosphate groups of two ADP molecules is geometrically equivalent with respect to the metal center. Regular hyperfine structure was not observed for the ATP complex due to inequivalent hyperfine couplings with phosphorus. ENDOR spectra of these complexes have shown, however, similar features assigned to the ³¹P coupling of 20.6 MHz only.¹⁷

In contrast, HYSORE spectra of VO-ATP contained ³¹P cross-peaks with estimated couplings of 14.8 and 9.0 MHz assigned respectively to the β- and γ-phosphorus atoms of ATP.³⁷ Additionally, Buy et al. also reported similar couplings for VO²⁺ used as a spin probe for the Mg²⁺ binding site of wild-type F1 ATPase (TF1).³⁷ In addition to the phosphorus couplings, the spectra exhibited coupling from two nitrogens: a histidine imidazole and a lysine terminal amine, both equatorially coordinated to the paramagnetic center. It bears mentioning, however, that both spectra shown in Figures 6 and 7 of ref 37 for the VO-TF1-ATP and VO-ATP complexes show evidence of a third pair of cross-peaks corresponding to weak phosphorus coupling, similar to what is observed in our VO-TPH spectra. This observation was probably not discussed due to the low intensity of these cross-peaks at the selected τ values.

ENDOR data would allow the selection of the relative signs of *a* and *T* from the two possibilities indicated in Table 1, at least for the strongest ³¹P coupling. The 18–20 MHz coupling observed in the powder EPR and ENDOR spectra of VO-ADP and VO-ATP most probably corresponds to the perpendicular component of the hyperfine tensors. The two sets of hyperfine constants derived from the analysis of the P₁ cross-peaks give $A_{\perp} = |a - T| = 17.6$ and 11.8 MHz, respectively. Of these two values, only the larger value, corresponding to opposite signs of *a* and *T*, approaches the reported EPR and ENDOR splittings.¹⁷

Proton Couplings. Proton hyperfine couplings for coordinated water and alcohol molecules in VO²⁺ complexes in single crystal,³⁸ powder,²⁸ frozen aqueous^{28,29,39,40} and alcohol^{41–43} solutions, as well as in frozen protein solution,⁴⁴ have been investigated in detail. These studies differ markedly in the reported data. The most complete and accurate single-crystal ENDOR study of [VO(H₂O)₅]²⁺ doped in Tutton salt lists the principal components of hyperfine tensors for all ligand protons and orientation of their principal axes correlated with the location relative to the metal.³⁸ The perpendicular principal values $|T|$ of anisotropic hyperfine tensors for the protons of equatorially coordinated waters vary within 4.6 ± 0.4 MHz.⁴⁵ The isotropic coupling magnitude is dependent on the orientation of the water molecule relative to the V–O(H) bond. Values as

high as 8.67 MHz have been reported for protons located most closely to the equatorial plane.³⁸

The ESEEM investigations,^{28,29,44} focused on the analysis of sum combinations, also allow direct measurement of $|T|$. These studies reported variations for the equatorial proton anisotropic couplings within the same range.

ENDOR studies of frozen solutions^{39,41,42} usually provide the splittings along directions parallel and perpendicular to the V=O axis, measured at the parallel or perpendicular hyperfine features of the CW EPR spectrum. These splittings are equal to the diagonal components of the proton hyperfine tensor in the coordinate system of the *g*-tensor and therefore differ from the principal values of these tensors because their principal directions do not, in general, coincide with the principal directions of the *g*-tensor. As a result, the couplings reported for equatorial protons in these studies cannot be directly compared with the values obtained from single-crystal ENDOR and ESEEM data.

On the basis of previously reported results,^{28,29,38,44} one can conclude that the value of $|T| = 4.29$ MHz, found in our work from the contour analysis of the H₁ cross-peaks, and confirmed by the corresponding shift of sum combination peaks, belongs to protons from equatorially coordinated water(s). Atherton and Shackleton³⁸ have stated that the *a* and *T* values for such protons typically have opposite signs with the anisotropic constant being negative, leading to the choice of *a* = 8.8 MHz and *T* = –4.3 MHz for the protons producing cross-peaks H₁. We have already mentioned, however, that the increasing deviation of the points from the straight line at the ridges of the cross-peaks may indicate a contribution from protons with the spread in isotropic hyperfine coupling of $\sim \pm 2$ MHz.

Conversely, according to all publications mentioned above, protons from axially coordinated water molecules typically possess *T* = 3.1–3.4 MHz and isotropic constants close to zero. This is due to a deviation of the principal directions of the axial protons from *g*-tensor axes of approximately 15°. Signals from this type of proton have been reported in the HYSORE spectra of [VO(ImH)₄]²⁺ (ImH = imidazole) in aqueous solution.⁴⁶ HYSORE spectra of this complex did not show cross-peaks with characteristics similar to H₁ because all four equatorial positions were occupied by imidazoles and only the axial position was filled with a water molecule. Our 2D ESEEM spectra do not provide any evidence for peaks that would correspond to axially bound protons, leading us to suggest that there is no axially coordinated water molecule in the VO-TPH complex and that some other group occupies this position.

The cross-peaks of H₂ and H₃ possess anisotropic couplings far less than the typical values for protons of water ligands, and, therefore, the protons producing them must have different origins. ENDOR spectra of VO²⁺ in frozen aqueous and alcohol solutions show the presence of couplings assigned to the proton involved in a hydrogen bond to the vanadyl oxo (V=O···H).⁴¹ The splittings $A_{\parallel} = 4.34$ MHz and $A_{\perp} = 1.40$ MHz have been reported for this proton.⁴¹ Calculated values of $A_{\parallel} = |a + 2T| = 4.8$ MHz and $A_{\perp} = |a - T| = 1.2$ MHz for proton H₃, based on the combination of *a* = 2.39 MHz and *T* = 1.22 MHz, are in good agreement with the earlier work.⁴¹ This supports the assignment of H₃ to the hydrogen-bonded proton attached to

(38) Atherton, N. M.; Shackleton, J. F. *Mol. Phys.* **1980**, *39*, 1471.

(39) van Willigen, H. *J. Magn. Reson.* **1980**, *39*, 37.

(40) Mulks, C. F.; Kirste, B.; van Willigen, H. *J. Am. Chem. Soc.* **1982**, *104*, 5906.

(41) Mustafi, D.; Makinen, M. W. *Inorg. Chem.* **1988**, *27*, 3360.

(42) Kirste, B. H.; van Willigen, H. *J. Phys. Chem.* **1983**, *87*, 781.

(43) Dikanov, S. A.; Evelo, R. G.; Hoff, A. J.; Tyryshkin, A. M. *Chem. Phys. Lett.* **1989**, *154*, 34.

(44) Gerfen, G. J.; Hanna, P. M.; Chasteen, N. D.; Singel, D. J. *J. Am. Chem. Soc.* **1991**, *113*, 9513.

(45) The actual hyperfine tensors of protons demonstrate rhombicity up to a value of $T_x/T_y \approx 0.84$. Therefore, $|T|$ was calculated as one-half of the maximum principal value.

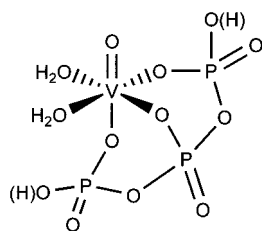
(46) Dikanov, S. A.; Samoilova, R. I.; Smieja, J. A.; Bowman, M. K. *J. Am. Chem. Soc.* **1995**, *117*, 10579.

the vanadyl oxygen particularly if only small deviations of the principal directions of its hyperfine tensor from the principal directions of g -tensor (as for protons of axial ligands) are suggested. Additional support for this argument is found in the behavior of the sum combination peaks. According to the estimates given above, the shift of the sum combination peak for H_3 has a value of ~ 0.06 MHz which is not detectable in the experimental spectra. Therefore, previous work based entirely on the analysis of sum combinations could not detect such a proton as we suggest here.

The parameters of the hyperfine tensor derived from the analysis of cross-peaks H_2 do not correlate with the values previously reported for the protons of ligands in the first coordination sphere discussed earlier. The anisotropic component $|T|$, in particular, is smaller than typical values obtained for both equatorial and axial ligands. It is likely that these peaks arise from one or more proton(s) bound as hydroxyls on the triphosphate ligand.

Structure of the Complex. The observations of three distinct hyperfine couplings from ^{31}P and of strong couplings from protons taken together indicate mixed coordination of VO^{2+} by phosphates and water molecules. The measured hyperfine couplings allow for some conclusions to be made about the structure of the complex(es).

The most intense proton peaks found in the HYSORE spectra belong to protons with hyperfine couplings typical for those of water molecules equatorially bound to the vanadyl ion.^{29,35,38} These protons also produce sum combination lines that can be observed in both the two-pulse and four-pulse ESEEM experiments. The shifts from the $2\nu_{\text{H}}$ matrix peak correspond exactly with the combination shifts observed previously^{28,29,44} for equatorial water molecules in VO^{2+} complexes. Comparison of the intensities of these combination peaks for VO-TPH with those for the aqua complex^{28,29} at different points of the EPR spectrum, including the $M_1 = -1/2$ "powder peak" as well as other components of hyperfine structure with g_{\parallel} and g_{\perp} , shows that, relative to the matrix peak at $2\nu_{\text{H}}$, the intensity of the shifted lines for VO-TPH is approximately one-half those observed for $[\text{VO}(\text{H}_2\text{O})_5]^{2+}$, suggesting that, for VO-TPH , there are two water molecules coordinated in the equatorial plane. From the data presented here, we propose a facial, tridentate triphosphate coordinated to the vanadyl ion, along with two water molecules located near to the equatorial plane.



Structurally, the variation of the hyperfine parameters for the three phosphorus atoms can be simply explained by the existence of different angles between the vanadyl oxo ($\text{V}=\text{O}$) and $\text{O}-\text{P}$ bonds. The isotropic constant is determined mainly by the unpaired spin density in the $3s$ orbital of each phosphorus atom. It is proportional to the value of 13 306 MHz, which is computed for unit spin density in this orbital.⁴⁷ In contrast, the anisotropic

coupling is the result of two factors: dipole–dipole coupling and indirect spin transfer. The value of the dipole–dipole contribution to the hyperfine tensor is determined chiefly by the $\text{V}-\text{P}$ distance, which should not change significantly between the different phosphorus atoms. The $\text{V}-\text{P}$ distance of 3.44 Å obtained through molecular modeling of phosphate coordination in VO-ADP complexes¹⁷ corresponds to $T = 0.79$ MHz in the point dipole approximation. Unpaired spin density in the $3p$ orbital determines the second contribution. The computed value for a $3p$ electron is 367 MHz, which is about 36 times less the value obtained for a $3s$ electron.⁴⁷ Therefore, the isotropic coupling is much more sensitive to structural variations than is the anisotropic coupling. One may expect that the maximum isotropic coupling belongs to the $\text{V}-\text{O}-\text{P}$ fragment closest to true equatorial coordination. Coupling magnitude is decreased with $\text{V}-\text{O}-\text{P}$ deviation from the equatorial plane. Similar behavior has been already found for protons of a VO-aqua complex where the isotropic coupling was close to zero for protons of an axial ligand and $\sim 5-9$ MHz for the protons of equatorial waters.³⁸ The anisotropic coupling values were much more stable, with a variation not exceeding 1.5 times.³⁸

The weak influence of an axial ligand on the characteristics of the EPR spectrum and the low spin density transfer on this ligand were confirmed recently by quantum-chemical calculations based on density functional theory of the $[\text{VO}(\text{H}_2\text{O})_5]^{2+}$, $[\text{VO}(\text{H}_2\text{O})_4]^{2+}$, and $[\text{VO}(\text{NH}_3)_4(\text{H}_2\text{O})]^{2+}$ complexes.⁴⁸ The calculations yielded anisotropic hyperfine coupling values of $|T| \approx 4$ MHz for equatorial protons and $|T| \approx 3$ MHz for axial protons with isotropic constants of $\sim 9-10$ MHz and ~ 0 MHz, respectively. Thus, these results generally support the assignment of the weakest phosphorus coupling as an axially ligated phosphate residue. However, a more complex mechanism of spin density distribution (which would require special consideration) probably takes place within the TPH molecule, including the transfer of spin density to the ^{31}P of the axially coordinated phosphate from the metal center through the axially coordinated oxygen as well as through the chain of equatorial $^{31}\text{P}-\text{O}$ donors. The latter mechanism is likely the major contributor to the observed ^{31}P isotropic constant of the axial phosphate.

For the VO-TPH model, the ratio of the anisotropic components of the ^{31}P hyperfine tensor for the equatorial ligands and axial ligand is equal to 1.3–1.7 and approximates the corresponding ratio of ~ 1.5 for equatorial and axial protons in the vanadyl–aqua complex. These values are also consistent with tridentate TPH coordination. In the case of bidentate equatorial coordination, the dipole–dipole contribution to $|T|$ from the ^{31}P of the noncoordinating phosphate decreases proportionally to $1/r^3$. An increase of the $\text{V}-\text{P}$ distance, even to 4.5–5 Å, as compared to 3.44 Å for a coordinated phosphate, would give $|T| = 0.25-0.35$ MHz instead of $|T| = 0.79$ MHz from the point dipole approximation. If the contribution to $|T|$ resulting from indirect spin density on the equatorial phosphates is estimated to be ~ 1 MHz, it can be suggested that the concomitant decrease of the anisotropic coupling constant of the noncoordinating phosphate would be proportional to the decrease of the isotropic coupling, found to be 5–7 times. Therefore, a roughly estimated value of $|T|$ for the third noncoordinating phosphate would not exceed ~ 0.5 MHz, thus

(47) Morton, J. R.; Preston, K. F. *J. Magn. Reson.* **1978**, *30*, 577.

(48) Carl, P. J.; Isley, S. L.; Larsen, S. C. *J. Phys. Chem. A* **2001**, *105*, 4563.

precluding only a bidentate coordination mode for the TPH ligand. This estimate is also linked to another possible model, involving monodentate coordination of a second TPH molecule to the axial position. In this case, the phosphorus nucleus of the noncoordinating O-P fragment of the equatorial TPH molecule as well as the two noncoordinating nuclei of the axial TPH would be present. Three dipole-coupled ³¹P nuclei, located at reasonable distances (4–5 Å) from the vanadyl ion, would produce a modulation of the Zeeman frequency of phosphorus in the time-domain two-pulse ESEEM with an amplitude of 0.01–0.04 depending on the magnetic field (related by H⁻²) and the distance to the nearest nucleus (*r*⁻⁶). The modulation of the proton Zeeman frequency in the time-domain two-pulse ESEEM has a value of about 0.25–0.30. These estimates of the modulation amplitudes and the intensity of the peak superimposed on the proton Zeeman frequency in the frequency-domain two-pulse ESEEM spectrum (Figure 1) allow for the prediction of an additional peak on the ³¹P Zeeman frequency with an intensity comparable to the intensities of the lines in the phosphorus doublet. There is, however, no evidence for such a peak on the ³¹P Zeeman frequency in the ESEEM spectra, even in those recorded at the lowest magnetic field component of the CW spectrum. The corresponding diagonal peak on the ³¹P Zeeman frequency is also absent in the HYSORE spectra as well, despite the suitability of HYSORE spectroscopy for the observation of low intensity peaks which are not clearly manifested in ESEEM spectra. Absence of these peaks, therefore, strictly limits the number of phosphorus nuclei surrounding the VO²⁺ to those producing the three observed splittings and allows the exclusion of bis(TPH) coordination.

Comparisons can be drawn between the VO-TPH system examined in this work and previous ENDOR¹⁷ and HYSORE³⁷ analyses of the VO-ATP system. HYSORE spectra of VO-ATP (at pH 6.3) and VO-TF1-ATP show three types of cross-peaks from ³¹P couplings similar to those observed in our case. In addition, two nitrogens in equatorial coordination positions were found in the VO-TF1-ATP complex, therefore suggesting equatorial coordination of phosphates to the two remaining sites. According to our data, the VO-TPH complex possesses two water molecules in these sites. The similarity between these results obtained from HYSORE spectra of three different complexes indicates a similar binding motif of one triphosphate chain with VO²⁺. Unfortunately, the HYSORE study of VO-ATP did not provide any information regarding the proton environment of the complex, which could have indicated directly the number of equatorial phosphate ligands.

Results reported in this work, however, do not agree with the conclusions reached in an ENDOR study of the VO-ATP system.¹⁷ Conclusions made about ATP coordination to VO²⁺ in ref 17 were based mainly on the similarity with a VO-ADP complex. There are, however, no detailed measurements of the magnitude and number of different hyperfine couplings from ³¹P nuclei, except some discussion of features assigned to the coupling at ~20 MHz. The presence of an axially coordinated water molecule follows from the observation of a 3 MHz coupling in the spectrum recorded at a perpendicular component of the hyperfine structure. This line disappears from the spectrum when CH₃OH/H₂O is replaced by CD₃OD/D₂O, but the EPR spectral line shape does not show a decrease upon such replacement. These conflicting observations may be a result of

pH differences and/or solvent effects due to the water/methanol mixtures used in the ENDOR study.¹⁷

The proposed structure is, to our knowledge, the first observed tridentate triphosphate coordination to the vanadyl ion, for either triphosphate or a triphosphate-containing ligand such as ATP. The axial phosphate interaction proposed from our results is of particular interest, as all other previous work with vanadyl has detected only equatorial phosphate coordination, corresponding to the β- and γ-phosphates of ATP. The proposed structure is consistent, however, with several crystal structures of other metal complexes with triphosphate (two containing Co(III)^{49,50} and one Cd(II)⁵¹) or ATP^{52–54} as tridentate ligands. Evidence also exists for the formation of a tridentate triphosphate Rh(III) complex from NMR spectroscopy and HPLC.⁵⁵ The triphosphate moiety is coordinated in a facial fashion, analogous to the structure proposed here.

Comparison to in vivo Coordination in Bone. The in vivo coordination structure of vanadyl ions in the bone mineral¹¹ is likely to be very similar to the type of triphosphate coordination observed in this study. The weak in vivo coupling of 3 MHz could indicate a solid-state axial phosphate interaction with the paramagnetic centers, while the two stronger couplings correlate very well with the two equatorial phosphate coupling constants determined in this work. Additionally, this model study has demonstrated that it is feasible for a single triphosphate moiety to generate three distinct vanadyl-phosphate coupling constants in a 1:1 solution complex between triphosphate and VO²⁺. Therefore, it is possible that, in the in vivo state, the vanadyl ions are coordinated in a relatively uniform fashion on the bone mineral surface. The two largest coupling constants of 15 and 9 MHz were found in both bone and VO-TPH and strongly suggest a bidentate phosphate motif in the equatorial plane in both samples. The presence of at least one water molecule (and likely two) correlates well with a previous study of vanadyl interactions with the bone mineral model compound hydroxyapatite.⁵⁶ Vanadyl ions did not incorporate into the apatitic lattice and could therefore be expected to interact strongly with the surrounding aqueous bilayer.⁵⁷

Conclusions

By utilizing advanced ESEEM and HYSORE spectroscopic techniques, the solution structure of the 1:1 triphosphate:vanadyl complex has been characterized. Contour line shape analysis determined three different vanadyl-phosphate couplings of 15, 9, and 1 MHz, the latter most likely corresponding to a weak axial interaction. This study, therefore, represents the first detection of a tridentate coordination mode for triphosphate in solution. Additionally, analysis of proton ESEEM and HYSORE peaks detected two water molecules coordinated equatorially on the vanadyl ions. Analysis of sum combination

(49) Haight, J. G. P.; Hambley, T. W.; Hendry, P.; Lawrence, G. A.; Sargeson, A. M. *J. Chem. Soc., Chem. Commun.* **1985**, 488.

(50) Merritt, E. A.; Sundaralingam, M. *Acta Crystallogr.* **1981**, B37, 1505.

(51) Lutsko, V.; Johansson, G. *Acta Chem. Scand. A* **1984**, 38, 415.

(52) Cini, R.; Burla, M. C.; Nunzi, A.; Polidori, G. P.; Zanazzi, P. F. *J. Chem. Soc., Dalton Trans.* **1984**, 2467.

(53) Butenhof, K. J.; Cochenour, D.; Banyasz, J. L.; Stuehr, J. E. *Inorg. Chem.* **1986**, 25, 691.

(54) Sabat, M.; Cini, R.; Haromy, T.; Sundaralingam, M. *Biochemistry* **1985**, 24, 7827 and references therein.

(55) Lin, I.; Knight, W. B.; Ting, S.-J.; Dunaway-Mariano, D. *Inorg. Chem.* **1984**, 23, 988.

(56) Vega, E. D.; Pedregosa, J. C.; Narda, G. E. *J. Phys. Chem. Solids* **1999**, 60, 759.

(57) Posner, A. S. *Clin. Orthop. Relat. Res.* **1985**, 200, 88.

lines from 1D four-pulse ESEEM spectra was instrumental in the assignment of the superimposed H₁ and H₂ cross-peaks. The determined coupling constants correlate very well with our earlier in vivo study, suggesting that, in bone, vanadyl ions are coordinated in a manner similar to that shown in our proposed structure.

The tridentate, facial coordination of triphosphate to VO²⁺ may have some implications in the study of the interactions of divalent metal ions with polyphosphate chains. Since most nucleotide:metal interactions studied in proteins have been found to be 1:1 and previous potentiometric studies of the Mg(II)–ATP system only detect formation of a 1:1 species,^{58,59} our study examining this monoligand complex may provide more applicable structural insights than previous studies that detected only 2:1 ATP:VO²⁺. The potential axial coordination of the ATP molecule may be important to substrate hydrolysis, especially when one considers that the native metal ion Mg²⁺ is more amenable to axial coordination due to the lack of a strong trans

oxo bond which weakens the sixth coordination site, and lack of any crystal field effects.⁶⁰

Acknowledgment. This paper is dedicated to Prof. Alan Davison, MIT, on the occasion of his 65th birthday. Acknowledgment is made to Kinetek Pharmaceuticals Inc., the Medical Research Council (now CIHR) of Canada, the Science Council of British Columbia (GREAT program, B.D.L.), and the Natural Sciences and Engineering Research Council of Canada for support of this work. ESEEM experiments were performed at the Department of Biophysics of Saarland University, Germany; the authors thank Professor Jürgen Hüttermann for the opportunity to perform this work, and S.A.D. is grateful to the Alexander von Humboldt Foundation for the support of his sojourn to Saarland University. The assistance of Dr. R. I. Samoilova during the experiments is appreciated.

JA011104S

(58) Shanbhag, S.; Choppin, G. *Inorg. Chim. Acta* **1987**, *138*, 187.

(59) Smith, R.; Martell, A.; Chen, Y. *Pure Appl. Chem.* **1991**, *63*, 1015.

(60) Cotton, F. A.; Wilkinson, G. *Advanced Inorganic Chemistry, A Comprehensive Text*, 4th ed.; John Wiley & Sons: Toronto, 1980.